THE ASTROPHYSICAL JOURNAL, 356:160–173, 1990 June 10

FAR-INFRARED, SUBMILLIMETER, AND MILLIMETER SPECTROSCOPY OF THE GALACTIC CENTER: RADIO ARC AND +20/+50 KILOMETER PER SECOND CLOUDS

R. GENZEL,[1] G. J. STACEY,[2] A. I. HARRIS,[1] C. H. TOWNES,[2] N. GEIS,[1] U. U. GRAF,[1]
A. POGLITSCH,[1] AND J. STUTZKI[1]

Received 1989 July 5; accepted 1989 December 13

ABSTRACT

We present far-infrared, submillimeter, and millimeter spectroscopic observations of the radio arc and the +20/+50 km s^{-1} molecular clouds in the Galactic center.

The spatial distributions of [C II] 158 μm and molecular line radiation and of the thermal radio continuum emission in the arched filaments of the radio arc are very similar. About 2×10^4 $M_\odot$, or 10% of the total gas mass in the radio arc, are contained in C^+ regions. The H^+/C^+ regions are probably located at the surfaces of the dense molecular clouds in the arc. Profiles, fluxes, and spatial distributions of the [C II] fine structure and CO rotational lines reported here, together with published intensities of the 63 μm [O I] line and of the mid-infrared, far-infrared, and radio continua, are very well matched by theoretical models for molecular clouds that are photoionized and photodissociated by stellar UV radiation. The line and continuum intensities do not fit available models in which the neutral interstellar clouds in the arc are ionized by shocks or by magnetohydrodynamic phenomena. The most likely interpretations are that OB stars have recently formed within and/or near the set of molecular clouds of the arc or that UV radiation reaches the arc from the Galactic center itself. This still leaves open the puzzle of the remarkable uniformity of the arc's ionization over scales of tens of parsec.

[C II] emission from the +50 km s^{-1} cloud (M-0.02–0.07) is substantially stronger than from the +20 km s^{-1} cloud (M-0.13–0.08). CO 7 → 6 and $C^{18}O$ 2 → 1 emission in the 50 km s^{-1} cloud comes from a narrow (3 pc) ridge at the eastern edge of the Sgr A radio source complex. Detection of blueshifted high-velocity $C^{18}O$ line emission toward the center of Sgr A East gives direct kinematic evidence for expanding gas motions associated with this nonthermal radio shell source. The energy of the explosion resulting in Sgr A East is estimated to be at least 8×10^{51} ergs. We conclude that the +20 and +50 km s^{-1} clouds are within 15 pc of the Galactic center. The +50 km s^{-1} cloud is compressed and accelerated by the expanding Sgr A East shell and may be exposed to the intense UV radiation from Sgr A West.

CO 7 → 6 emission from the clouds near the Galactic center and in the radio arc is relatively weak. Either the high temperatures and densities derived from NH_3 and CS observations may not be characteristic of the bulk of the molecular gas, or the high filling factor low-J ^{12}CO emission does not come from the bulk of the clouds, but from warm, low-density interclump gas.

Subject headings: galaxies: The Galaxy — galaxies: nuclei — infrared: sources — interstellar: molecules

I. INTRODUCTION

Within about 10′ of Sgr A*, the compact radio source at the dynamical center of the Galaxy, there are several large, molecular and ionized gas clouds. Figure 1 shows an overview of the region. Contours of 2.8 cm radio continuum (Pauls *et al.* 1976) delineate the locations of the Sgr A complex and the "radio arc" region about 10′ north of it. In the radio arc region, one commonly distinguishes the straight, nonthermal filaments approximately perpendicular to the Galactic plane ($l \approx 0.^\circ16$) and the arched, thermal filaments (or the "bridge") that appear to connect the northwestern part of the straight filaments with the Galactic plane near $l \approx 0.05^\circ$ (Yusef-Zadeh, Morris, and Chance 1984). There are several prominent peaks in the chains of thermal filaments. They are usually referred to by their Galactic coordinates (e.g., G0.07+0.04, etc.). The thermal filaments of the radio arc are associated with a set of dense molecular gas clouds at negative LSR velocities (v_{LSR} = −10 to −50 km s^{-1}). These clouds appear not to participate in galactic rotation and probably have significant noncircular velocities (Bally *et al.* 1987; Serabyn and Güsten 1987).

A massive ($M_{gas} \approx$ a few 10^5 $M_\odot$) molecular cloud with LSR velocity near +20 km s^{-1} is located about 3.′5 southeast of Sgr A* (M-0.13−0.08; e.g. Güsten, Walmsley, and Pauls, 1981). The +20 km s^{-1} cloud appears to be connected with a second cloud at v_{LSR} = 40 to 50 km s^{-1} (M-0.02−0.07) located ≈3′ northeast of Sgr A*.

The location, physical conditions, and excitation of the Galactic center molecular clouds are not well understood. Are the molecular clouds as close to the Galactic center as their projected distances seem to indicate? And if so, are they physically associated with the Sgr A radio sources and the circumnuclear gas ring (cf. Brown and Liszt 1984; Genzel and Townes 1987)? Most important, how are the gas clouds heated and ionized? One possibility is that OB stars have formed relatively recently ($\leq 10^6$ yr) near the center and are now photoionizing clouds in their vicinity.

An alternative interpretation is that the filaments in the radio arc trace large-scale magnetic field lines and are ionized by fast shocks, plasma waves, or magnetic flux tubes (Yusef-Zadeh 1986; Sofue and Fujimoto 1987; Heyvaerts, Norman,

[1] Max-Planck-Institut für extraterrestrische Physik, Garching, FRG.
[2] Department of Physics, University of California, Berkeley.

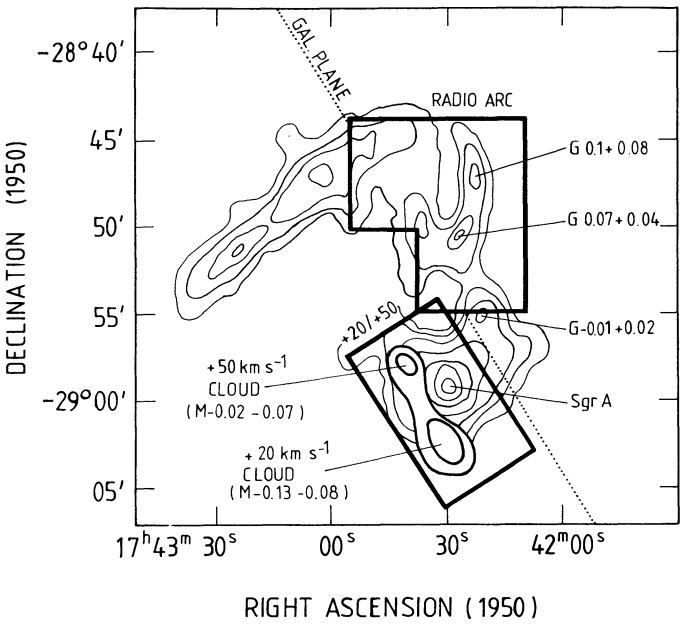

FIG. 1.—Overview of the Galactic center region. The two regions mapped in the 158 μm $^2P_{3/2} \rightarrow {}^2P_{1/2}$ [C II] line are indicated by boxes marked "RADIO ARC" and "+20/+50." Thin contour lines mark the distribution of 2.8 cm radio continuum from the work by Pauls *et al.* (1976:1′ beam). Prominent continuum sources are designated. Heavy contours mark the location of the +20 and +50 km s^{-1} clouds.

and Pudritz 1988; Morris and Yusef-Zadeh 1990). To explore these questions, we have investigated the excitation, spatial distributions, and dynamics of the circumnuclear environment by observations and mapping of the 158 μm $^2P_{3/2} \rightarrow {}^2P_{1/2}$ fine structure line of singly ionized carbon, of the 372 μm $J = 7 \rightarrow 6$ and 867 μm $J = 3 \rightarrow 2$ rotational transitions of ^{12}CO, and of the 1.37 mm $J = 2 \rightarrow 1$ transition of C^{18}O. For simpler comparison with earlier work, we adopt a Sun-Galactic center distance of $R_\odot = 10$ kpc. At this distance 1′ equals 3 pc. The best current estimate for $R_\odot$ is near 8 kpc (Reid 1989), and all distances, masses, and luminosities may be scaled accordingly.

The organization of this paper is as follows. After discussing the observations in § II, we present the results of the different measurements as well as first interpretations in the following two sections: first for the radio arc region (§ III) and then for the +20/+50 km s^{-1} clouds (§ IV). In § V we analyze the impact of our new measurements on the interpretation of the physical conditions, excitation and heating of the gas clouds in the arc and near the center.

II. OBSERVATIONS

a) Far-Infrared Observations

Far-infrared observations of the $^2P_{3/2} \rightarrow {}^2P_{1/2}$ transition of [C II] at 157.7409 μm were taken on the NASA Kuiper Airborne Observatory in 1988 June with the Mark II University of California, Berkeley, cryogenic Fabry-Perot spectrometer (Lugten 1987). We employed a three-element linear array of stressed Ge:Ga detectors (Stacey *et al.* 1989) with a FWHM spatial resolution of 55″ (solid angle 9×10^{-8} sr) and a spacing of 55″ between detectors along position angle 120°. The spectral resolution was fixed at 67 km s^{-1} (FWHM), and the system noise equivalent power (NEP) was 3 to 4×10^{-15} W Hz$^{-1/2}$, including all instrumental, telescope, and atmospheric losses. The telescope's secondary chopped at 33 Hz with a 5′ amplitude. We first took spectra at selected positions in the radio arc and the +20/+50 km s^{-1} clouds. Next, we fixed the Fabry-Perot spacing to pass the strongest emission in either region (−40 km s^{-1} in the arc and +40 km s^{-1} in the clouds). In the radio arc region, three fully sampled raster maps were made with 11 × 12 points (R.A. × decl.) at a spacing of 30″. The integration time per point was about 4 s, resulting in a 3 σ sensitivity of 10^{-4} ergs s^{-1} cm^{-2} sr^{-1}. The three maps necessary to cover the region of the arched, thermal filaments of the arc overlap. The region mapped is marked by the L-shaped boundaries in Figure 1. The northeastern map had its reference beam east, the other two west of the signal beam. The line-to-continuum ratio is large, so there is no significant correction for the underlying continuum. However, spectra taken in the northeastern region show some contamination due to emission in the reference beam, presumably because there is strong line emission at positive velocities near the Galactic plane. In the region of the +20 and +50 km s^{-1} clouds, one raster map was made with 9 × 20 points in Galactic latitude and longitude coordinates with 30″ spacing. The reference beam was 5′ southeast, in the direction of decreasing Galactic latitude. In the two sets of maps, data from the off-center detectors were used to extend the map boundaries and check on the consistency of the data. The absolute pointing accuracy of the maps is better than about ±15″. Absolute line intensities were made by observing the continuum of Sgr A (1.5×10^3 Jy: Crawford *et al.* 1985) and of W51 IRS 2 (1.5×10^4 Jy: Thronson and Harper 1979). The calibration is accurate to ±30%.

Submillimeter Observations

Submillimeter spectra of the CO $J = 7 \rightarrow 6$ transition at 371.6474 μm (806.6517 GHz) were taken toward the arc and +20/+50 km s^{-1} clouds in 1988 July with the 3.8 m United Kingdom Infrared Telescope on Mauna Kea and the Max-Planck-Institut für extraterrestrische Physik (MPE) Cassegrain, Schottky heterodyne spectrometer (Harris *et al.* 1987). The receiver temperature was about 4000 K (DSB) and the FWHM beam size was 26″. The backend was a dual acousto-optical spectrometer covering an instantaneous bandwidth of 1.1 GHz (380 km s^{-1}). The telescope's secondary switched at 2 Hz between the source position and a position 180″ east and west. The absolute pointing accuracy was about ±5″. We determined the submillimeter transmission and line temperature calibration in the way described by Harris (1986). The zenith transmission in 1988 July varied around 45%. All CO line temperatures are Rayleigh-Jeans main beam brightness temperatures; that is, antenna temperatures corrected for line-of-sight atmospheric transmission and divided by main beam efficiency (0.31). The temperature scale is correct to ±30%.

c) Near-Millimeter Observations

Observations of the 1.365411 mm (219.5603 GHz) C^{18}O $2 \rightarrow 1$ and the 866.963 μm (345.796 GHz) ^{12}CO $3 \rightarrow 2$ transitions toward radio arc and +50 km s^{-1} cloud were made in 1989 March with the IRAM 30 m telescope. The FWHM beam sizes were 14″ at 1.4 mm and 9″ at 867 μm. For the 1.4 mm observations, we used the IRAM SIS receiver ($T_{DSB} \approx 300$ K; Blundell, Carter, and Gundlach 1988). At 867 μm we employed the new MPE 350 GHz SIS receiver ($T_{DSB} \approx 900$ K; Harris *et al.* 1989). In both cases the spectrometer was a bank of 512 × 1 MHz filters. The data were taken in position-switched and/or sky-chopped mode (amplitude 4′ in telescope azimuth). The

system was calibrated by the chopper wheel method and by observations of the planets and the Moon. Line temperatures given below are, again, Rayleigh-Jeans main beam brightness temperatures, antenna temperatures corrected for line-of-sight transmission (typically 60% at 1.4 mm and 22% at 867 μm) and main beam efficiency (0.45 at 1.4 mm and 0.2 at 867 μm from observations of Jupiter, diameter 36″). The temperature scale is correct to about $\pm 25\%$ at 1.4 mm and $\pm 30\%$ at 867 μm.

III. RESULTS: RADIO ARC

a) *Spatial Distribution of* [C II] *Line Emission*

There is strong 158 μm [C II] fine structure line emission at LSR velocities between -70 and -10 km s^{-1} over the entire area mapped (Fig. 2; [Pl. 5]). The far-infrared line emission is well correlated with the radio continuum and molecular line emission in the arched, thermal filaments (right side of Fig. 2; Yusef-Zadeh 1986; see also Pauls *et al.* 1976; Serabyn and Güsten 1987). The [C II] emission has peaks on or near the far-infrared continuum sources and H II regions G0.07+0.04 and G-0.01+0.02 (see Table 1). Two ridges extend north from G0.07+0.04 along the two prominent sets of radio filaments in the arc (Fig. 2) and with a secondary peak near G0.1+0.08. The [C II] emission toward the straight, nonthermal filaments is much weaker. A slight increase of [C II] flux near the northeastern map boundary (17^h43^m, $-28°48'$) may be due to the H II region G0.18−0.04 near the center of the nonthermal filaments (Yusef-Zadeh 1989). The spatial correlation of the [C II] emission with the radio continuum and molecular emission is not perfect, however. Wherever the radio continuum is significantly offset from the CS $2 \rightarrow 1$ emission mapped by Serabyn and Güsten (1987), the [C II] emission is also not coincident with the radio continuum and appears to peak between radio and molecular emission (e.g., the vicinity of G0.07+0.04). The most likely interpretation, already put forward by Serabyn and Güsten (1987), is that the ionized gas is at the surfaces of the dense molecular clumps delineated by the CS emission. The [C II] emission may come from partially ionized interfaces between the fully molecular and fully ionized zones.

b) *Spatial Distribution of* CO *Emission*

Bally *et al.* (1987, 1988) and Serabyn and Güsten (1987) have demonstrated that the arched filaments are closely associated with a system of dense molecular clouds. To study the relationship between molecular and ionized gas at high spatial resolution we took ^{12}CO $3 \rightarrow 2$ and C^{18}O $2 \rightarrow 1$ spectra with the IRAM 30 m telescope in steps of 14″ along a 45° position angle from the peak of the far-infrared continuum emission of G0.07+0.04 (Table 1) toward the northeast. The integrated line fluxes of ^{12}CO $3 \rightarrow 2$ and C^{18}O $2 \rightarrow 1$ along this cut are also shown in Figure 3. The positions of G0.07+0.04 and of two of the long filaments of the arc which the cut crosses at about right angles are also indicated. Clearly the H II region complex and far-infrared continuum peak G0.07+0.04 is a major concentration of molecular gas column density and mass ($\sim 2 \times 10^4\ M_\odot$). The two ionized filaments appear to be very near to or coincident with secondary peaks of ^{12}CO $3 \rightarrow 2$ and C^{18}O $2 \rightarrow 1$ emission, indicating that they too are local maxima of gas column density [$N(H_2) \sim 8 \times 10^{22}$ cm^{-2}, see below].

c) *Luminosity and Mass of* C^+ *Regions*

The [C II] emission in the arc has an integrated brightness (10^{-3} ergs s^{-1} cm^{-2} sr^{-1}) that comes close to that of the circumnuclear disk surrounding Sgr A West. The line brightness temperatures may even be larger than in Sgr A ($T_{\rm Planck} \approx 30$ K) because the lines in the arc are less than half as wide as the circumnuclear disk's (cf. Fig. 4). Compared with the emission in Sgr A itself, the arc is therefore more prominent in [C II] line emission than in either the radio or infrared continua. This is shown more quantitatively in Table 1. On the peak near G0.07+0.04, the line luminosity per 1′ beam is about 450 $L_\odot$, or about 0.1% of the 25 to 130 μm far-infrared luminosity measured by Gatley *et al.* (1977, 1978). Here we have assumed that the arc is at the distance of the Galactic center. This ratio is comparable to that which is found in many OB star-forming regions in the Galaxy. Integrated over the map in Figure 2, the [C II] line luminosity is about $10^4\ L_\odot$, or about a factor of 2 to 3 greater than the circumnuclear disk's [C II] luminosity (Genzel *et al.* 1985; Lugten *et al.* 1986).

A lower bound to the peak column density of C^+ ions is about 8×10^{17} cm^{-2}. The actual column density will be higher if the hydrogen density is less than about 3×10^3 cm^{-3}, the critical density of the C^+ $^2P_{3/2}$ level, and if the kinetic temperature is not much larger than $h\nu/k = 91$ K (see Crawford *et al.* 1985). The ratio of [C II] line flux to the [O I] 63 μm line flux measured by Erickson *et al.* (1989) is about 1, indicating hydrogen densities in the C^+ zones of a few 10^3 cm^{-3}. With this density and an assumed kinetic temperature of 200 to 300

TABLE 1

COMPARISON OF CONTINUUM AND LINE EMISSION IN THE RADIO ARC AND SAGITTARIUS A WEST

	Sgr A West	G0.07+0.04	G0.01+0.02	G0.1+0.08
R.A. =	$19^h42^m29^s.3$	$17^h42^m26^s.2$	$17^h42^m22^s$	$17^h42^m22^s.5$
Decl. = (1950)	−28°59′19″	−28°51′45″[c]	−28°55′10″	−28°47′40″
25–130 μm, luminosity[a] (1′ beam, 1 = $2.3 \times 10^5\ L_\odot$)	10	3.2	2.7	1.3
2.8 cm radio continuum[b] (1′ beam, 1 = 0.3 Jy)	10	1	1	0.3
158 μm [C II] intensity (55″ beam, 1 = 2×10^{-4} ergs s^{-1} cm^{-2} sr^{-1})	10	6	6	3.4

NOTE.—The listed position is the peak of [C II] line and far-IR continuum emission; the radio continuum peak is about 40″ northeast.

[a] Gatley *et al.* 1977, 1978.

[b] Pauls *et al.* 1976.

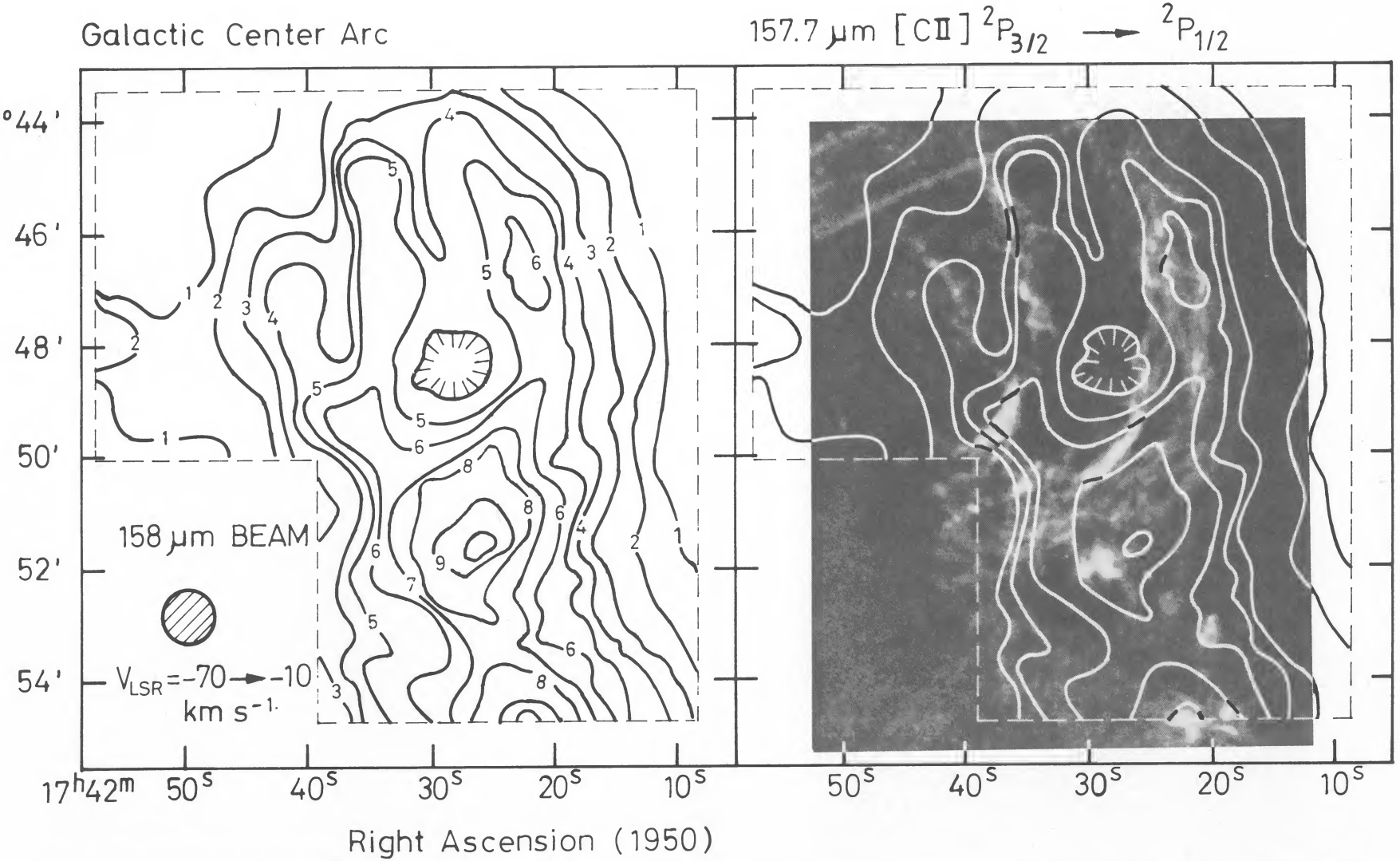

FIG. 2.—[C II] map of the radio arc region between $v_{LSR} = -70$ and -10 km s^{-1}. The [C II] beam is 55″ (FWHM) and the maps were made on a 30″ grid in R.A. × decl. (see text). *Left*: [C II] map. Contour unit is 1.2 × 10^{-4} ergs s^{-1} cm^{-2} sr^{-1}; *right*: selected [C II] contours superposed on a radiograph of a 6 cm continuum VLA map by Yusef-Zadeh (1986: resolution 4″ × 3″).

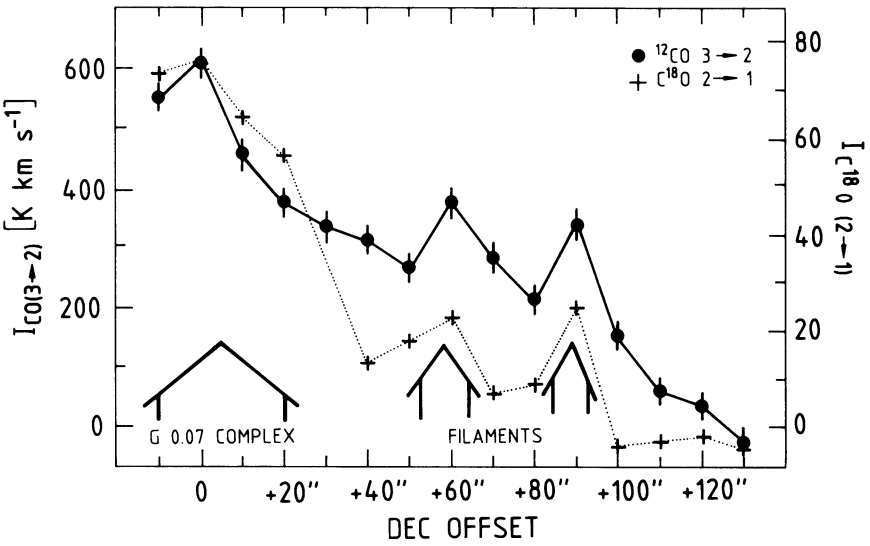

FIG. 3.—Cut of integrated C^{18}O 2 → 1 (beam 14″) and ^{12}CO 3 → 2 (beam 9″) flux along position angle 45° east of north. The base position is at R.A. = 17^{h}42^{m}26^s.2, decl. = −28°51′45″ (1950). Multiply the decl. offset by 1.4 to get the full spatial offset along the cut. Marked at the bottom are the approximate locations of the far-infrared continuum/H II region complex G0.07 + 0.04 and of two of the prominent, narrow filaments of the arc which the cut crosses at about right angles (cf. Yusef-Zadeh 1986).

K which is typical of most other [C II] sources in the Galaxy (Genzel, Harris, and Stutzki 1989), a more accurate estimate of the peak C^+ column density is about 2.5 times larger than the lower bound given above [$N(C^+) \approx 2 \times 10^{18}$ cm^{-2}]. That factor would even be larger if the [C II] emission were optically thick. With a C^+/H_2 fractional abundance ratio $\leq 3 \times 10^{-4}$, the hydrogen mass per beam in the C^+ region around G0.07 + 0.04 is 500 $M_\odot$ or more. Integrated over the map of Figure 2, we estimate a hydrogen mass of about 1 to 2 × 10^4 $M_\odot$ in the C^+ regions of the arc. Table 2 compares these values with those of the ionized and molecular gas components in the radio arc. The main result is that densities, column densities, and masses in the C^+ zones are about an order to magnitude larger than those of the ionized gas, and about an order of magnitude less than those of the molecular gas. These relative proportions are comparable to many OB star-forming regions in the Galaxy. In these regions the [C II] emission comes from dense photodissociation regions associated with molecular clouds and excited by the far-ultraviolet radiation from embedded and external OB stars (e.g., Genzel, Harris, and Stutzki 1989).

d) CO 7 → 6 *Emission and Line Profiles*

Two CO 7 → 6 spectra were taken, one near G0.07 + 0.04, and one near G0.18 − 0.04 (the so-called "pistol," Yusef-Zadeh 1989). The CO 7 → 6 line was detected at the former position and its spectrum is displayed in Figure 4 along with a [C II] spectrum and profiles of the H110α and CS 2 → 1 lines (Yusef-Zadeh 1986; Serabyn and Güsten 1987). ^{12}CO and C^{18}O 3 → 2 spectra toward the same position are displayed in Figure 5.

The FWHM line widths near G0.07 + 0.04 range between 30 and 45 km s^{-1} for the various tracers (Fig. 4). Our C^{18}O 2 → 1 spectrum (Fig. 5) and the CS profiles of Serabyn and Güsten (1987) indicate that the overall profile may be a superposition

TABLE 2

DENSITIES, COLUMN DENSITIES, AND MASSES IN RADIO ARC[a]

Component	n(H, H_2) [cm^{-3}]	N(H + 2H_2) [cm^{-2}]	M(H, H_2) [$M_\odot$]
Ionized gas	400 to 1000[b]	10^{21} (1′)	60 (1′)
			1.5 × 10^3 (integrated over arc)
C^+ regions	~3 × 10^3[c]	≥8 × 10^{21}	≥5 × 10^2 (1′)
		(1′)[d]	≥1.5 × 10^4 (integrated)
Molecular gas	10^4[e]	4 → 15 × 10^{22}	4 → 20 × 10^3 (1′)[f]
		(1′)[f]	≈2 × 10^5 (integrated)

[a] For a 1′ diameter region centered on the far-infrared peak of G0.07 + 0.04.

[b] From 52/88 μm [O III] line ratio (Erickson *et al.* 1989) or from radio emission measure and size (Yusef-Zadeh *et al.* 1984).

[c] From ratio of [C II] flux to [O I] 63 μm flux (Erickson *et al.* 1989); see discussion of derivation of densities from [O I]/[C II] ratios in Watson (1984), Genzel *et al.* (1985).

[d] $[C^+]/[H] \leq 3 \times 10^{-4}$.

[e] Average of model calculations of CO emission (this paper) and CS excitation (Serabyn and Güsten 1987).

[f] Lower value from 50 μm optical depth of warm dust ($\tau_{50\mu m} \approx 0.05$, Gatley *et al.* 1977, 1978) and $N(H) = 8 \times 10^{23}\ \tau_{50}$; upper value from CO model calculations (this paper) and $[CO]/[H_2] = 8 \times 10^{-5}$, $[CO]/[C^{18}O] = 250$.

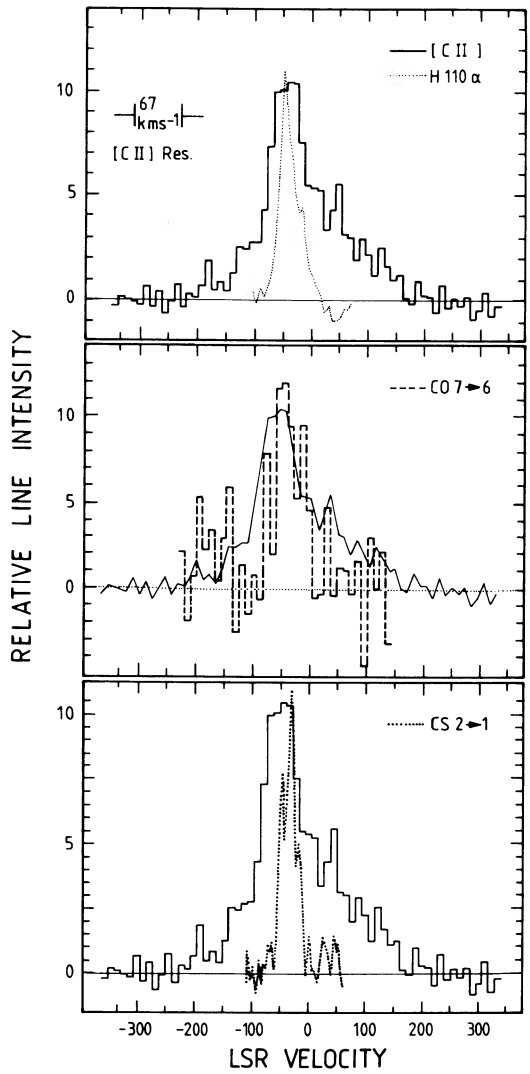

FIG. 4.—Comparison of spectra near G0.07+0.04 (R.A. = $17^h42^m26^s.2$, decl. = −28°51′45″). The centroid of the radio continuum emission of G0.07+0.04 is about 30″ to 60″ farther north. The [C II] profile (histogram in top panel, 67 km s^{-1} FWHM resolution with Lorentzian profile) in a 55″ beam is shown in all three panels, together with the H110α spectrum (*top*: 22″ × 11″ beam, Yusef-Zadeh 1986), the CO 7 → 6 profile (*middle*: 26″ beam, this paper, peak Rayleigh-Jeans brightness temperature 6.5 K), and the CS 2 → 1 spectrum (*bottom*: 25″ beam, Serabyn and Güsten 1987).

of several components of 10 to 15 km s^{-1} width. Allowing for the differences in spectral resolution and signal-to-noise ratios, there is no evidence that the higher excitation CO 7 → 6, [C II] and H110α lines are much wider than low-J ^{12}CO lines. The ^{12}CO lines are somewhat (20%) wider than the $C^{18}O$ and CS lines. The [C II] and H110α lines toward G0.07+0.04 are blue-shifted by about 10 to 15 km s^{-1} relative to the CO and CS lines, indicating streaming motions between ionized and molecular gas. Inspection of the CS spectra by Serabyn and Güsten and the H110α spectra of Yusef-Zadeh (1986) indicates that in most other locations of the thermal filaments, velocity shifts between neutral and ionized gas are less than about 5 to 10 km s^{-1}. In addition to [C II] emission associated with the radio arc ($v_{LSR} \sim -10$ to -60 km s^{-1}), the [C II] profile in Figure 4 also shows emission at positive LSR velocities which is almost certainly associated with other clouds along the line of sight to the Galactic center.

e) Molecular Gas in the Arc: Model Calculations

The ^{12}CO 7 → 6 line emission toward G0.07 + 0.04 is relatively weak (T_{mb} = 7 K). This is surprising, since observations of 1.2 cm inversion lines of NH_3 and mm transitions of high density tracing molecules (like CS) show moderately intense extended emission, and have been interpreted as indicating high gas densities and moderately high temperatures [$n(H_2) \approx$ 2 to 5 × 10^4 cm^{-3}, $T_{kin} \approx$ 50–100 K, Güsten *et al.* 1985; Güsten, Walmsley, and Pauls 1981; Serabyn and Güsten 1987; Bally *et al.* 1987).

In order to quantify the physical parameters of the molecular gas in the arc, we have constructed simple one-component models that account for the combined effects of non–LTE excitation, radiative transport, and clumpiness of the gas. Martin, Sanders, and Hills (1984) have shown that only models taking into account clumping can satisfactorily match the observed line intensities *and* line widths of various CO isotopic transitions. Our "clumpy cloud" model is described in more detail in Appendix A. Table 3 lists the observed ^{12}CO and ^{13}CO 1 → 0 line brightness temperatures and widths taken from the literature, along with our new ^{12}CO 2 → 1, 3 → 2, and 7 → 6 and $C^{18}O$ (2 → 1) data (Fig. 5) for G0.07+0.04. Table 3 also gives the parameters of a typical one component, clumpy cloud model that gives an acceptable fit to the line intensities and widths (labeled Low-Temperature, Low-Density). We have assumed fractional abundance ratios [^{12}CO]/[^{13}CO] = 25, [^{12}CO]/[$C^{18}O$] = 250 that are probably representative of the Galactic center region (e.g., Wannier 1980).

The low intensity of the CO 7 → 6 line means that only models of relatively low molecular hydrogen density ($\lesssim 10^4$ cm^{-3}) and kinetic temperature ($\lesssim$40 K) come close to fitting all ^{12}CO, ^{13}CO, and $C^{18}O$ data. In order to demonstrate the fact that models with parameters suggested by the NH_3 and CS data fail to explain the CO measurement we show a second

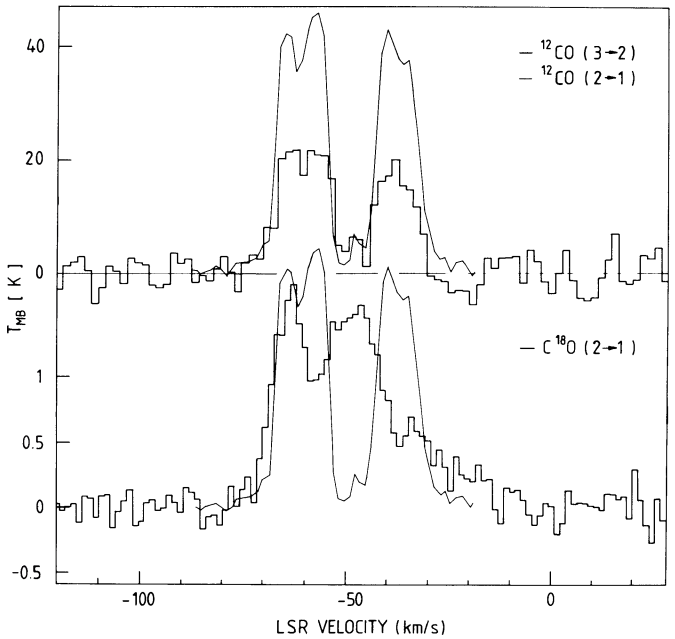

FIG. 5.—$C^{18}O$ 2 → 1, ^{12}CO 2 → 1, and 3 → 2 spectra toward G0.07+0.04 (same position as in Fig. 4). The $C^{18}O$ and ^{12}CO 2 → 1 data were taken in position-switched mode with the IRAM 30 m telescope, the ^{12}CO 3 → 2 data with the wobbler.

TABLE 3

OBSERVED AND DERIVED PARAMETERS OF CO EMISSION IN ARC

	Observations Radio Arc: G0.07+0.04	Low-Temperature, Low-Density Model[a]	High-Temperature, High-Density Model[b]
^{12}CO 1→0	T_{mb} = 20 K (21″)	T = 20 K	4 K
	Δv(FWHM) = 35 km s^{-1}	Δv = 35 km s^{-1}	33 km s^{-1}
	Serabyn and Güsten (87)	τ = 15	6
^{12}CO 2→1	40 K (26″)	26 K	6 K
	37 km s^{-1}	39 km s^{-1}	35 km s^{-1}
		47	20
^{12}CO 3→2	20 K (30″)[c]	24 K	7 K
	37 km s^{-1}	40 km s^{-1}	36 km s^{-1}
		76	38
^{12}CO 7→6	7 K (26″)	7 K	7 K
	≈45 ± 10 km s^{-1}	37 km s^{-1}	36 km s^{-1}
		26	53
^{13}CO 1→0	3.5 K (100″)	4.5 K	0.4 K
	35 km s^{-1}	32 km s^{-1}	31 km s^{-1}
	Bally *et al.* (87)	1	0.2
C^{18}O 2→1	1.5 K (25″)	1.4 K	0.2 K
	30 km s^{-1}	31 km s^{-1}	31 km s^{-1}
		0.8	0.1

[a] Clumpy cloud model (see text) with T_{kin} = 40 K, $n(H_2) = 3 \times 10^3$ cm^{-3}, Gaussian clumps with FWHM; Δv_{clump} = 10 km s^{-1}, Δv_{cloud} = 30 km s^{-1}, beam area filling factor ϕ_A = 0.20, peak total CO column density in a clump N_{cl}(CO) = 10^{19} cm^{-2}, [^{12}CO]/[^{13}CO] = 25, [^{12}CO]/[C^{18}O] = 250.

[b] Clumpy cloud model with T_{kin} = 80 K, $n(H_2) = 3 \times 10^4$ cm^{-3}, Gaussian clumps with Δv_{clump} = 15 km s^{-1}, Δv_{cloud} = 30 km s^{-1}, ϕ_A = 0.02, N_{cl}(CO) = 2×10^{19} cm^{-2}.

[c] Data were taken in Spatial-Chopping mode (4′ Wobbler).

model in Table 3. This model (labeled High-Temperature,-High-Density) is for a hydrogen density of 3×10^4 cm^{-3} and a kinetic temperature of 80 K, and uses a very small filling factor (0.02) that is adjusted to give a good match to the ^{12}CO 7→6 temperature. It fails to account for all other lines by factors between 5 and 9, however. A homogeneous cloud model of small filling factor can simulate the ratio of the ^{12}CO 7→6 to the ^{13}CO 1→0/C^{18}O 2→1 line intensities (as the filling factor does not depend on optical depth), but fails to explain the low-J ^{12}CO line intensities.

The fact that the most prominent C^{18}O peak in Figure 5 is coincident with a deep self-absorption feature in the low-J ^{12}CO lines indicates the presence of gas with very low kinetic temperatures (≤10 K), or gas with a combination of low temperatures and low densities. Neither of the two models (or any other single component model) can account for the puzzling difference in brightness of the low-J ^{12}CO lines (20 K for 1→0, 40 K for 2→1, and 20 K for 3→2). These facts indicate that the low-J ^{12}CO emission may come from a medium with a complex density and temperature structure, and will be discussed in more detail in a forthcoming paper (Genzel *et al.* 1990).

With an assumed CO/H_2 ratio similar to that in the disk of the Galaxy (8×10^{-5}), we derive a peak integrated molecular hydrogen column density of 1.5×10^{23} cm^{-2} in a 1′ beam centered on G0.07+0.04. The molecular hydrogen mass in this region then is about 2×10^4 $M_\odot$. The total molecular mass integrated over the entire arc region is about 10 times larger, or about 2×10^5 $M_\odot$ (from the CS map of Serabyn and Güsten 1987). Our mass estimate is about 3 times less than that inferred by Serabyn and Güsten (1987) on the basis of their CS observations and an assumed [CS]/[H_2] ratio of 3×10^{-9}. Our estimates are about 5 times larger than the gas column densities and masses estimated from the 50 μm continuum data by Gatley *et al.* (1977, 1978): τ_{dust}(50 μm) ≈ 0.05, the dust emissivity law by Hildebrand (1983), and a gas-to-dust ratio of 10^2. A likely reason for this discrepancy is that the 50 μm emission comes from relatively warm dust ($T_d \approx 50$ K). A large fraction of the total dust mass may be cooler and thus not contributing significantly to the 50 μm emission. The derived densities, column densities, and masses are listed in Table 2 for comparison with the parameters of the ionized gas and C$^+$ regions.

IV. RESULTS: +20 AND +50 km s^{-1} CLOUDS

a) [C II] *Mapping*

The distribution of [C II] line radiation between v_{LSR} = +10 and +70 km s^{-1} is given in Figure 6, along with an overlay of the [C II] contours on a map of 1 mm continuum emission from Mezger *et al.* (1986). Except in the immediate vicinity of Sgr A*, the 1 mm continuum emission traces the column density of dust, and hence probably the column density of the gas in the bulk of the cloud. As in the case of the radio arc region, the [C II] emission is moderately intense (peak 9×10^{-4} ergs s^{-1} cm^{-2} sr^{-1}) over most of the region mapped. There are two emission peaks. The most prominent one at $\Delta l \approx 40''$ is coincident with the redshifted "lobe" of the rotating, circumnuclear ring surrounding Sgr A*/IRS 16 and has been discussed previously by Lugten *et al.* (1986). The second maximum is close to the peak of the +50 km s^{-1} molecular cloud (M-0.02−0.07) and several compact H II regions just east of the nonthermal radio shell of Sgr A East (Ekers *et al.* 1983). Weaker [C II] emission appears to be extended over the entire diameter of the +50 km s^{-1} cloud. The [C II] intensity decreases gradually toward the +20 km s^{-1} cloud. The map and an individual spectrum taken toward the peak of the +20 km s^{-1} cloud show that the [C II] flux is at least 6 times weaker there than toward the +50 km s^{-1} cloud.

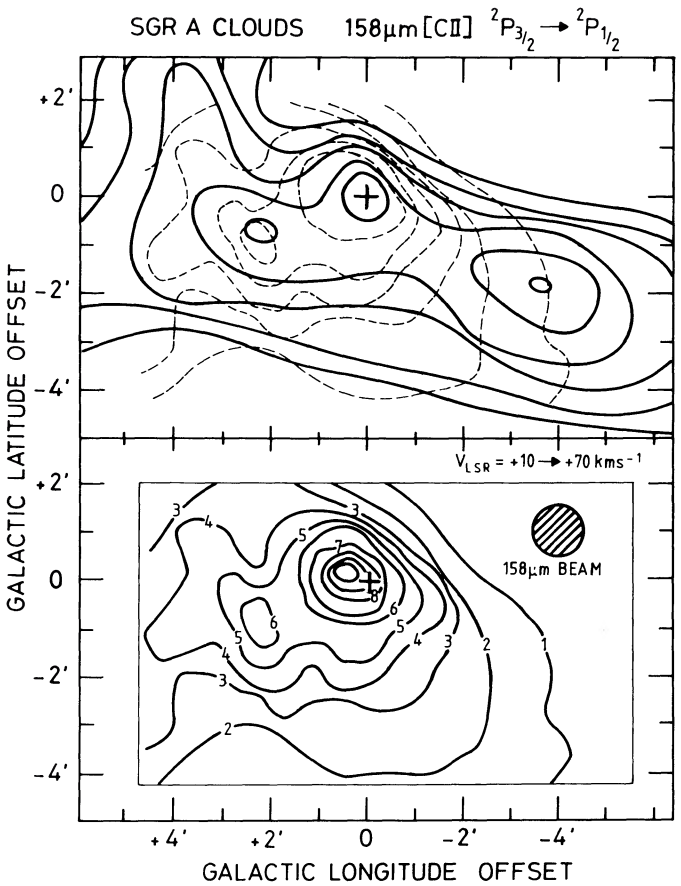

FIG. 6.—[C II] maps of the +20/+50 km s^{-1} clouds. *Bottom*: Contours of [C II] emission between LSR + 10 and +70 km s^{-1}. Contour unit is 1.4 × 10^{-4} ergs s^{-1} cm^{-2} sr^{-1}, resolution 55″. The maps were made on a 30″ grid in Galactic latitude × longitude. The cross marks the position of Sgr A*/IRS 16. *Top*: Selected [C II] contours (*dashed*) superposed on contours of 1.3 mm continuum emission from Mezger *et al.* (1986, 90″ beam). The left and right, 1.3 mm continuum peaks are identical with the peak positions of the +50 and +20 km s^{-1} molecular clouds.

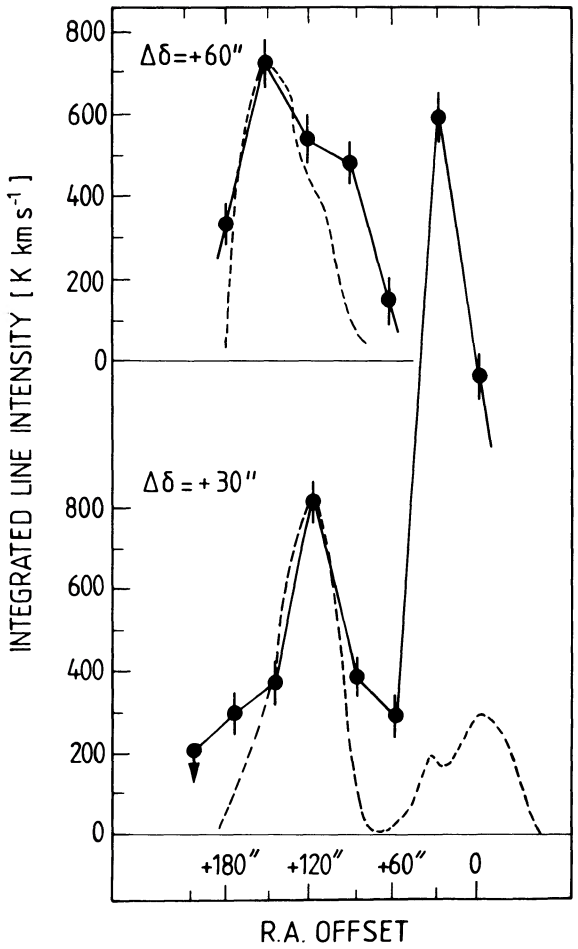

FIG. 7.—Cuts of CO 7 → 6 integrated line flux through the +50 km s^{-1} cloud. The two cuts are east–west, at declination offsets Δδ = +30″ (*bottom*) and Δδ = +60″ (*top*) relative to Sgr A*/IRS 16 (R.A. = 17^{h}42^{m}29^s.3, decl. = −28°59′18″ (1950)). The CO 7 → 6 data points (*filled circles*, 25″ beam) were taken every 30″. Dashed curves indicate schematically the distribution of 1.3 mm continuum flux from Mezger *et al.* (1989, 13″ beam). The strongest CO 7 → 6 peak at Δα ≈ +30″ is the northern, redshifted lobe of the circumnuclear disk (Harris *et al.* 1985). The second peak at Δα ≈ 120″ → 150″ is the +50 km s^{-1} cloud. The sharp eastern edge of the Sgr A East nonthermal radio source is at Δα = 100″ at Δδ = 30″ and Δα = 80″ at Δδ = 60″.

b) CO 7 → 6 *Mapping*

Figure 7 shows the velocity integrated intensity of the CO 7 → 6 emission along two east–west cuts through the peak of the +50 km s^{-1} cloud, Sgr A East and the redshifted lobe of the circumnuclear ring, together with corresponding cuts of 1 mm dust emission from the paper by Mezger *et al.* (1989). In addition to strong submillimeter CO emission from the circumnuclear disk (Harris *et al.* 1985), the new data show a well-defined, sharp increase of submillimeter CO emission on a ridge coincident with the eastern edge of Sgr A East. Location and diameter of the enhanced line emission are remarkably similar to those seen in 1 mm continuum.

Figure 8 shows an average CO 7 → 6 spectrum in about a 1′ diameter region toward the peak of the +50 km s^{-1} cloud, along with a ^{13}CO 1 → 0 spectrum from the same region (Armstrong and Barrett 1985). The 7 → 6 line is relatively weak when compared to the 1 → 0 and 2 → 1 lines, as in the arc. The spectra have about the same linewidth, but the 7 → 6 profile has a significant central depression, either due to foreground absorption by cooler gas or as a result of the fact that the 3′ chopper throw was not sufficient to chop off the source. The 7 → 6 line toward the +20 km s^{-1} cloud has about the same intensities but has no indication of a central depression.

c) C^{18}O *Mapping*

Figure 9 is a map of the velocity-integrated C^{18}O 2 → 1 emission of the +50 km s^{-1} cloud, which should trace the total molecular column density. The strongest C^{18}O emission arises from a north-south ridge just at the eastern edge of Sgr A East (Fig. 9*b*) and is similar to the distribution of the CO 7 → 6 line and 1.3 mm continuum emission from cold dust (Mezger *et al.* 1989). The C^{18}O line emission tapers off slowly across the face of Sgr A East and toward Sgr A*. Previous molecular absorption observations (Güsten and Downes 1980; Brown and Liszt 1984; Sandqvist *et al.* 1987) have indicated that this part of the +50 km s^{-1} cloud is mostly in front of Sgr A East. From the integrated C^{18}O flux and [C^{18}O]/[H$_2$] ≈ 3 × 10^{-7}, we estimate a peak molecular hydrogen column density of the 50 km s^{-1} cloud of 6 × 10^{23} cm^{-2} and a molecular hydrogen mass of about 2 × 10^5 $M_\odot$ integrated over the map. This is in reasonable agreement with the data of Mezger *et al.* [1989: $N(H_2) \approx 3 \times 10^{23}$ cm^{-2}].

Figure 10 is a C^{18}O spectrum taken at offset (Δα,

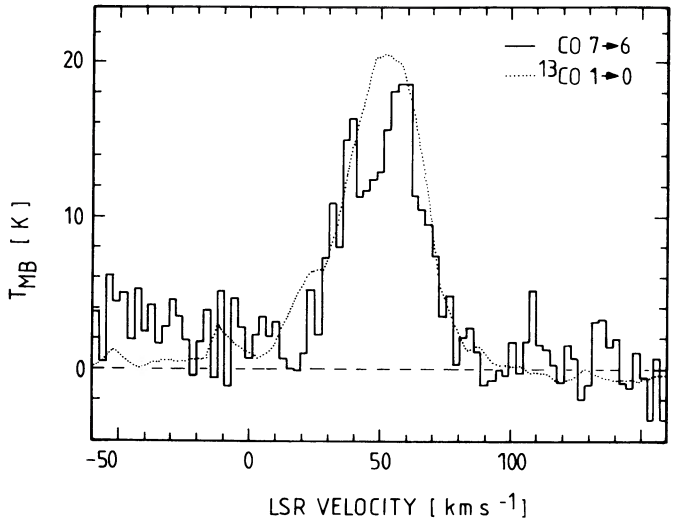

FIG. 8.—Comparison of CO 7 → 6 (*histogram*) and ^{13}CO 1 → 0 (*dotted*, Armstrong and Barrett 1985) profiles toward the peak of the +50 km s^{-1} cloud. In order to compare data with the same beam size, the CO 7 → 6 profile is an average of spectra over a 1′ diameter region. Multiply the temperature scale by 0.72 to obtain main beam brightness temperatures for the ^{13}CO 1 → 0 line.

$\Delta\delta) = (+100'', +40'')$ from Sgr A*, just inside the Sgr A East shell. In addition to strong emission from the 50 km s^{-1} cloud, there is high-velocity C^{18}O emission between $v_{LSR} = -80$ and +20 km s^{-1} that show up as a continuous wing on the blue-shifted side of the emission from the 50 km s^{-1} cloud. Figure 9 shows that this high-velocity emission can be seen across most of the face of Sgr A East, is strongest toward its center, but is weak or below detectability away from Sgr A East. An east–west position-velocity cut at Δdecl. = +40″ is shown in Figure 11. The high-velocity C^{18}O emission has its largest velocity extent toward the center of Sgr A East (ΔR.A. ≈ +80″) and diminishes quickly toward the center of the +50 km s^{-1} cloud. There are other, well-known kinematic features in the Galactic center that have negative velocities. These features (3 kpc arm at −50 km s^{-1}, expanding molecular ring at −120 km s^{-1}, and a component at −30 km s^{-1}) all have distinct velocities, however, and are spatially very extended. We thus conclude that the spatially concentrated blueshifted feature discussed above is associated with Sgr A East.

The new C^{18}O 2 → 1 and CO 7 → 6 data thus clearly indicate that the +50 km s^{-1} cloud is directly associated with Sgr A East, that it physically interacts with it, and that gas related to Sgr A East is expanding at high velocity. We discuss the implications in § V*b* below.

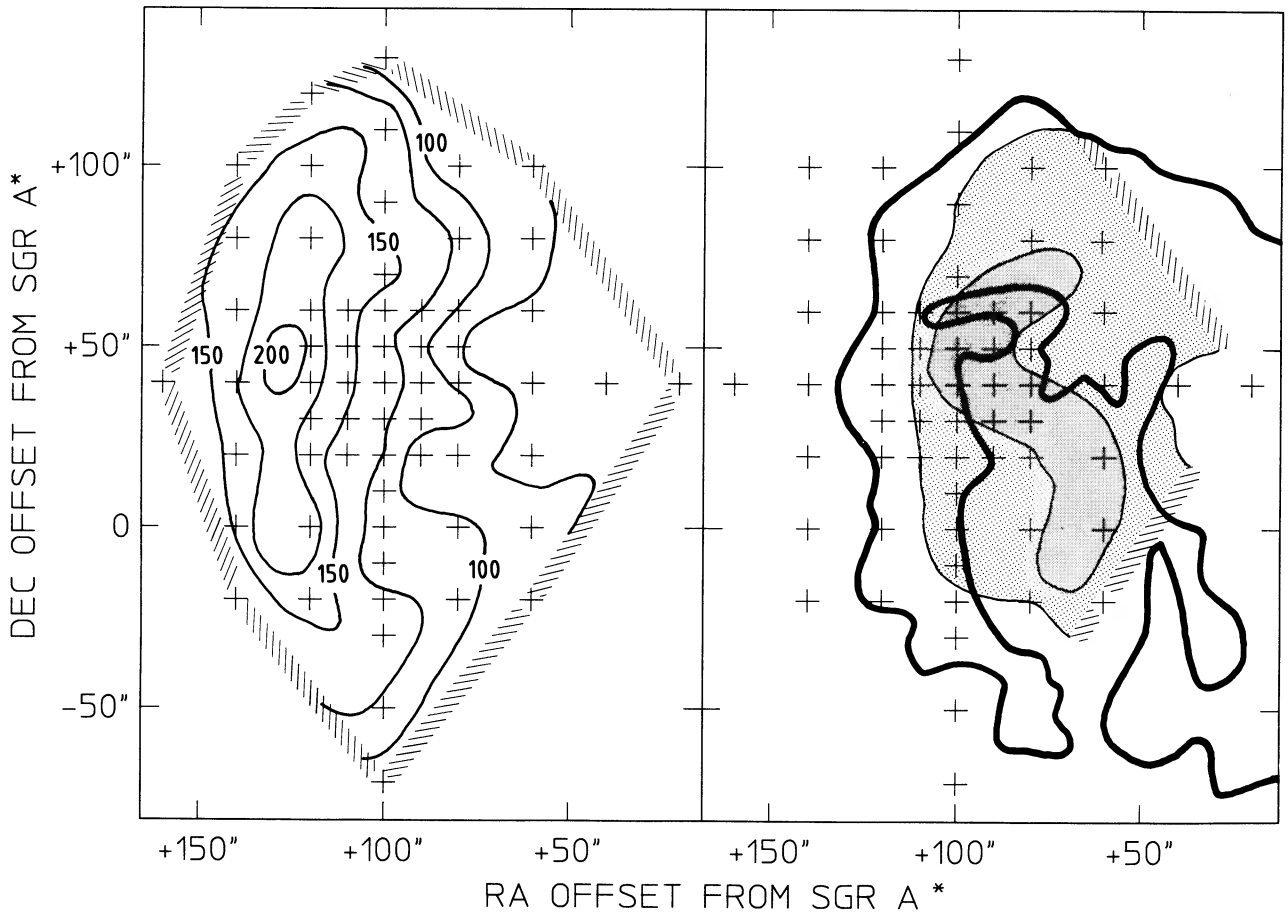

FIG. 9.—Distribution of C^{18}O 2 → 1 emission in the +50 km s^{-1} cloud (14″ beam). (*a*, *left*): Map of integrated C^{18}O line flux between LSR +30 and +70 km s^{-1}. Contour units are km s^{-1} times degree K main beam brightness temperature. The spatial offsets are relative to Sgr A* ($17^h42^m29^s.3$, −28°59′18″). Crosses mark the positions where data were taken. The map is not fully sampled. (*b*, *right*): Schematic of the distribution of the nonthermal radio continuum emission of Sgr A East (Ekers *et al.* 1983; *heavy lines*). Stippled region denotes the area where blueshifted high-velocity C^{18}O emission ($v_{LSR} = -80$ to +20 km s^{-1}) was detected. Solid black marks the area of strong blueshifted high-velocity C^{18}O emission.

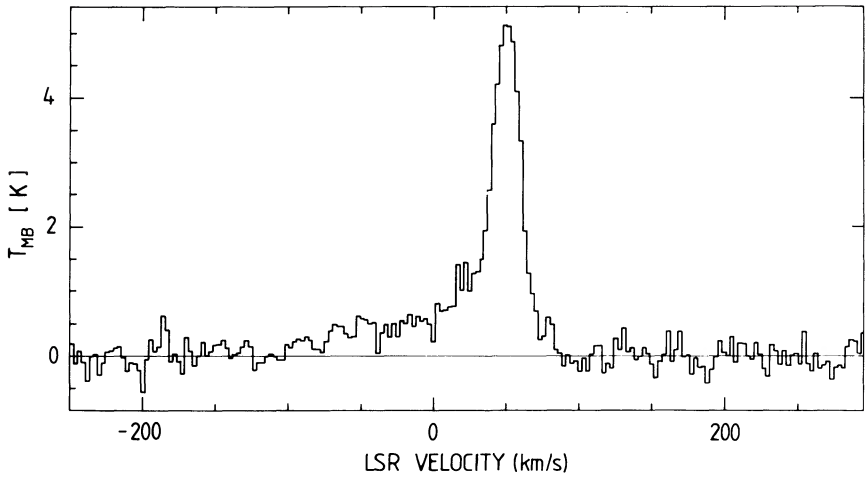

FIG. 10.—$C^{18}O$ 2 → 1 profile at offset (ΔR.A., Δdecl.) = (+100″, +40″) from Sgr A*

V. DISCUSSION

a) What Ionizes the Thermal Filaments in the Radio Arc?

The system of thermal and nonthermal filaments in the radio arc is a remarkable phenomenon. On geometrical and morphological grounds, Yusef-Zadeh (1986) and Morris and Yusef-Zadeh (1990) concluded that the thermal filaments are not photoionized H II regions excited by the ultraviolet radiation of nearby or embedded OB stars. The main argument is the uniformity of the ionization along a rather long path (several 10 pc). Serabyn and Güsten (1987) have argued that photoionization by UV radiation from the Galactic center can also be excluded geometrically. A number of other possible ionization mechanisms have been considered (see Morris and Yusef-Zadeh 1990 for a more detailed summary). Yusef-Zadeh (1986) and Bally *et al.* (1988) proposed fast shocks in cloud-cloud collisions. Sofue and Fujimoto (1987) invoked a magnetized jet of supersonic, thermal gas emanating from the galactic nucleus. Heyvaerts, Norman, and Pudritz (1988) proposed that magnetic loops, created near Sgr A*, collide with the molecular clouds in the arc region and ionize them. Most recently, Morris and Yusef-Zadeh (1990) have argued that the gas is ionized by Alfvén's (1954) "critical ionization" effect, which is caused by the magnetohydrodynamic interaction of a rapidly moving cloud with a strong ambient magnetic field.

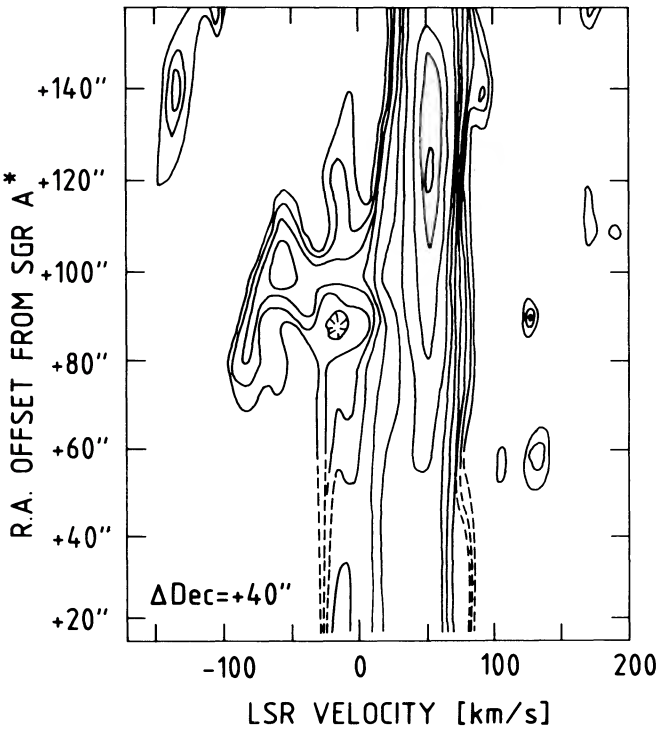

FIG. 11.—Position-velocity diagram of $C^{18}O$ emission along an east-west line through Sgr A East and the 50 km s^{-1} cloud. All offsets are relative to Sgr A*.

Valuable new information on the characteristics and physical conditions of the gas clouds in the radio arc is now available from the absolute and relative continuum and line fluxes that have been reported in this paper and in Erickson *et al.* (1989). We now discuss how this information can be used to better determine the possible ionization mechanisms in the arc.

i) *Photoionization versus Shock Models*

Table 4 summarizes several of the directly observed or derived parameters of the gas and dust emission in the region around G0.07 + 0.04 at the southern end of the arc. This particular region is well studied, and other regions in the arc, such as G0.1 + 0.08, appear to have comparable characteristics. Also listed are the theoretically expected values of these parameters for the cases of a 40 km s^{-1}, pure gas dynamic (*J*-type) shock for two different preshock densities, taken from the recent *J*-shock models by Hollenbach and McKee (1989). This is the largest shock velocity that is still consistent with the observed widths of the CO 7 → 6, [C II], and H110α lines. A larger shock velocity can, of course, be consistent with the data if the shock propagation direction is at a large angle with respect to the line of sight. While that could possibly be the case over a small region, it is unlikely to be applicable over such a large and complex region as the radio arc.

The magnetosonic speed of the ions is 20 to 80 km s^{-1} for the range of ion densities (400 to 1000 cm^{-3}, Table 2) and magnetic fields (100 to 1000 μG) likely present in the arc. Since this velocity may be larger than the shock velocity, a magnetohydrodynamic (*C*-type, Draine 1980) shock has to be con-

TABLE 4

OBSERVED PARAMETERS OF G0.07+0.04 vs. SHOCK AND PDR MODELS

Parameter	Observed	J-Shock[a] $n_0 = 10^3$ $v_{shock} = 40$ km s^{-1}	J-Shock[a] $n_0 = 10^4$ $v_{shock} = 40$ km s^{-1}	H II + PDR[b] $\epsilon_0 = 10^3 \rightarrow 10^4$ $\epsilon_{interstellar}$ $n_H = 10^3$ cm^{-3} $L_{UV} = 10^6 L_\odot$
[C II] Intensity (ergs s^{-1} cm^{-2} sr^{-1})	1.2×10^{-3}	2×10^{-5}	2×10^{-5}	10^{-3}
[O I]/[C II] Intensity ratio	1[c]	$10 \rightarrow 20$	≥ 100	$0.5 \rightarrow 2$
CO $7 \rightarrow 6$ Intensity (ergs s^{-1} cm^{-2} sr^{-1})	1.5×10^{-4}	$10^{-7} \rightarrow 10^{-6}$	6×10^{-6}	10^{-6}
EM (cm^{-6} pc)	5×10^5 (1′)[d] $\rightarrow 5 \times 10^6$ (10″)	200[e]	3×10^3	EM and flux consistent with L_{UV} and n_e
n_e (cm^{-3})	≈ 300[e]	$\geq 10^3$	$\geq 10^4$	$\leq 10^3$
T_e (K)	$5000 \rightarrow 7000$[f]	$\approx 10^4$	$\approx 10^4$	≥ 6600[g]
$S(10\,\mu m)/S(5\,GHz)$	$10 \rightarrow 30$[h]	...	...	$5 \rightarrow 50$[i]
L_{Lines}/L_{TOT}	0.002	≈ 1	≈ 1	0.005

[a] Hollenbach and McKee 1989, n_0 is preshock density of hydrogen nuclei in cm^{-3}.
[b] Photodissociation region (PDR) models from Hollenbach, Tielens, and Takahashi (1989), $\epsilon_{interstellar} = 1.6 \times 10^{-3}$ ergs cm^{-2} s^{-1}.
[c] Erickson *et al.* 1989.
[d] Pauls *et al.* 1976.
[e] Yusef-Zadeh 1986.
[f] From line to continuum ratio in H110α recombination line of Yusef-Zadeh 1986.
[g] Wink *et al.* 1983.
[h] Yusef-Zadeh *et al.* 1989.
[i] Genzel *et al.* 1982.

sidered as well. One of the main characteristics of a *C*-type shock is that the peak postshock temperature is much smaller than in a *J*-shock (a few 10^3 K instead of $>10^5$ K). *C*-shocks thus produce little ionization (Draine, Roberge, and Dalgarno 1983; Chernoff, Hollenbach, and McKee 1982). As far as column densities of ionized gas is concerned, the *J*-shock numbers in Table 4, therefore, represent the "best case."

In the last column of Table 4 we list the theoretical predictions (from the models by Hollenbach, Tielens, and Takahashi 1989 and A. Sternberg 1989, private communication) for a combination of an H II region around a few late-type O or early B stars of total UV luminosity similar to the far-IR luminosity of G0.07+0.04 ($\sim 10^6\ L_\odot$), plus a photodissociation region (PDR) exposed to a far-UV radiation intensity of 10^3 to 10^4 times the local interstellar radiation field. That intensity corresponds to the dilution of a UV luminosity of about $10^6\ L_\odot$ at half the diameter of G0.07+0.04 (a few pc). We implicitly assume in this model that the UV radiation from a few distributed OB stars within or near G0.07+0.04 ionize and photodissociate gas at the surfaces and edges of the molecular clouds in their vicinity.

The interpretation of Table 4 appears straightforward. A standard photoionization/photodissociation model explains almost all observed parameters without difficulty. The *J*-shock models fail to account for the absolute and relative line intensities and emission measures by one to three orders of magnitude and cannot account at all for the infrared continuum. The observed bright, spatially extended [C II] fine structure line emission in the radio arc is probably the most unambiguous indicator that an intense ($\epsilon_{uv} \geq 10^3\ \epsilon_{interstellar}$) far-ultraviolet radiation field must be present. The shock models are also not able to account for the [O III] fine structure line emission observed by Erickson *et al.* (1989). Neither shock nor PDR models account for the CO $7 \rightarrow 6$ line flux. The $7 \rightarrow 6$ CO emission most likely comes from a larger column density of somewhat cooler molecular gas deeper into the cloud, as in the models presented in Table 3.

ii) *Origin of the Far-Infrared Luminosity*

Morris and Yusef-Zadeh (1990) have proposed that the far-infrared continuum radiation from the radio arc is due to dust heating in the general radiation field from the extended cluster of late-type stars centered on the Galactic nucleus (Becklin and Neugebauer 1968). The luminosity density of the late-type stars at a distance of 20 pc from the center is about $10^3\ L_\odot/pc^3$, as derived from the luminosity profile of Sanders and Lowinger (1972). Considering a region of radius 1′ centered on G0.07+0.04, the late-type stars within and outside that volume may contribute about 1 to $2 \times 10^5\ L_\odot$. Most of the stellar radiation emerges at visible and near-infrared wavelengths where the dust absorption efficiency is lower than in the UV. Even if all of the radiation impinging on the cloud is absorbed by the dust in G0.07+0.04, it fails the observed 30 to 120 μm luminosity of G0.07+0.04 ($\sim 10^6\ L_\odot$) measured by Gatley *et al.* (1977, 1978) and Dent *et al.* (1982) by about a factor of 5 to 10, and the total luminosity by more. Furthermore, heating by the visible/near-infrared radiation from the late-type stars cannot explain the relatively high dust temperatures of G0.07+0.04 (~ 50 K, Gatley *et al.* 1977). The intensity of the stellar radiation field is about 1 erg s^{-1} cm^{-2}. With a dust absorption efficiency scaling as λ^{-1}, we derive a dust temperature between 20 and 33 K from this stellar radiation field intensity, depending on the absolute value of the absorption efficiency in the visible and near-infrared. We conclude that the luminosity of G0.07+0.04, and, by analogy the other peaks in the thermal radio arc cannot be accounted for by the late-type stars. Heating by late-type stars may, however, significantly contribute to the more extended far-infrared emis-

sion near the Galactic center (Cox and Laureijs 1989), in agreement with the discussion in Morris and Yusef-Zadeh (1989).

iii) *Critical Ionization Mechanism*

As a fast-moving neutral cloud moves into a region containing a strong, rigid magnetic field, the charged particles in the cloud start gyrating about the field lines, while the neutrals are initially unaffected. If the velocity of the cloud is large enough ($\geq$40 km s^{-1}), collisions between ions and neutrals can then lead to cascade ionization which may eventually ionize the entire cloud surface (Morris and Yusef-Zadeh 1989). Although detailed calculations of the energy balance and thermal structure in a zone heated by this "critical ionization mechanism" (Alfvén 1954) are not available, the following general considerations speak against this mechanism as the dominant one for the ionization of the clouds in the arc. First, in a critical ionization front, as in shocks, the ionized and partially ionized gas are downstream from the interaction point between cloud and magnetic field. As a result, the ionized and partially ionized gas must be at least as dense as the upstream molecular gas since the cooling time scales (1 to 10 yr at the densities in the arc) are much smaller than dynamical time scales (>1000 yr). Such a density structure of the gas is not observed in the arc (Table 2), however. The molecular gas appears to be much denser than the ionized gas. The densities of ionized, partially ionized, and neutral gas components listed in Table 2 are derived from line ratios. They should be more reliable than densities inferred from emission measures or column densities (Morris and Yusef-Zadeh 1989). Second, the velocity of the ionized gas should be significantly different from that of the neutral gas, as the ionized gas is approximately at rest with respect to the magnetic field in these models. For instance, in the specific model of Morris and Yusef-Zadeh (1989), one would expect a velocity shift of up to 100 km s^{-1} between neutral and ionized gas. Again, such a large shift is not observed (see § III*d*). Third, the scenario of a fast-moving cloud colliding with a "rigid" magnetic field "wall" used by Morris and Yusef-Zadeh (1989) will inevitably lead to a *C*- or *J*-shock. Table 4 showed that a *J*-shock of velocity consistent with the observed line width fails to account for the observed emission measure of ionized gas and [C II] flux by orders of magnitude. It appears reasonable to us that the same will be true for the critical ionization mechanism. Finally, the critical ionization mechanism also cannot account for the total energy output in the far-infrared continuum, and the discussion of the last section on the origin of the far-infrared continuum radiation is relevant here as well.

In summary, the indicators of the excitation of the ionized, partially ionized and neutral gas and dust, taken together, are perfectly consistent with ordinary photoionized molecular clouds. Ionization by fast shocks or by the critical ionization effect are not consistent with these data. We have not addressed the magnetic loop model of Heyvaerts, Norman, and Pudritz (1988), as Serabyn and Güsten (1987) and Morris and Yusef-Zadeh (1989) already discussed several reasons why that model cannot account for the ionization in the radio arc.

The most likely interpretation of the observations of line and continuum emission is thus that several tens of OB stars have in fact formed recently within or along the thermal filaments of the arc. In order to be consistent with the spatial distribution and the remarkable uniformity of the ionization of the thermal filaments, these OB stars must be distributed more or less smoothly along the filaments or, alternatively, there must be a cluster of hot stars near the geometrical center of the arc. The possibility of UV radiation reaching the arc from the center itself has to be reconsidered as well. In the latter cases it is necessary that the gas density near the stars is low so that most of the ionizing photons can reach the clouds of the arc. It is then an important question how these OB stars are related to the molecular cloud associated with the arc. These conclusions *can be tested* by direct observation of the hot, luminous stars in the near- or mid-infrared. We note that a quintuplet of compact 2 to 10 μm sources associated with G0.18$-$0.04 (the "pistol") has recently been found by Okuda *et al.* (1989).

iv) *Remarks on the Connection of the Radio Arc with Sagittarius A*

Between the southern end of the arched, thermal filaments near G0.07+0.04 and the northern end of the halo of Sgr A near the compact H II region G-0.01+0.02 there is a significant drop in the brightness of spatially extended radio continuum emission. There is thus no evidence from the radio continuum maps that the arc is linked to the Galactic nucleus (Morris and Yusef-Zadeh 1989). In contrast, the molecular observations by Serabyn and Güsten (1987) and Bally *et al.* (1987) clearly show that negative velocity gas clouds stretch south of G0.07+0.04 (decl. = $-28°51'$) to within 1′ of Sgr A*, and may continue past Sgr A to decl. = $-29°20'$. The minimum of radio continuum emission between $-28°52'$ and $-28°55'$ corresponds to a maximum of molecular column density. Our [C II] map also shows intense emission in this declination range. Lugten *et al.* (1986) have previously reported intense, extended [C II] emission at $v_{LSR} \approx -35$ km s^{-1}, 1′ to 3′ northeast of Sgr A. We propose that the set of blueshifted gas clouds with which the thermal radio filaments are associated physically connect to the center of the Sgr A region. The presence of only a few compact H II regions and the lack of extended radio emission south of $-28°51'$ may be a direct result of the high gas column densities and correspondingly small penetration lengths for Lyman continuum photons. On the other hand, the extended filamentary radio emission north of decl. = $-28°51'$ could also indicate that the mean gas densities are low in the vicinity of these filaments.

b) Relationship of the +20/+50 km s^{-1} Clouds to Sagittarius A

Our new $C^{18}O$ 2 → 1 and CO 7 → 6 measurements strongly support the conclusion of Mezger *et al.* (1989) that the +50 km^{-1} cloud is physically related to the Sgr A complex (see also Goss *et al.* 1989). The bulk of the cloud is adjacent to the nonthermal source Sgr A East and partly wraps around it. The narrow ridge of the +50 km s^{-1} cloud adjacent to Sgr A East probably indicates that the cloud has been compressed by the expanding radio shell source. We interpret the blueshifted high-velocity $C^{18}O$ emission as molecular material originally in the +50 km s^{-1} cloud that has now been accelerated to velocities $\sim$100 km s^{-1} by the expansion of Sgr A East.

The detection of high-velocity $C^{18}O$ emission allows a first estimate of the kinetic energy of the expanding material. From the $C^{18}O$ high-velocity line flux (50 K km s^{-1}) and spatial extent we infer about $2 \times 10^4\ M_\odot$ of high-velocity gas. With an average velocity of about 100 km s^{-1} relative to the quiescent 50 km s^{-1} cloud, the kinetic energy is about 2×10^{51} ergs. As the observed high-velocity gas only covers about 25% of the entire solid angle around Sgr A East, approximately 8×10^{51} ergs are required to account for the high-velocity motions, and more if radiation losses are included. Sgr A East is probably the manifestation of a recent ($t \leq$ a few 10^5 yr) explosion in the

Galactic center whose total energy was equivalent to that of at least several supernovae.

Lugten *et al.* (1986) and Mezger *et al.* (1989) have given several reasons why Sgr A East and hence, the $+50$ km s^{-1} clouds may be *in* the Galactic center and may be associated with Sgr A West. If the $+50$ km s^{-1} cloud is within 10 pc of the center, as indicated by its projected distance, radiation from Sgr A West itself may substantially contribute to the UV field impinging on the cloud's surface. In fact, if UV radiation from the center can escape toward the $+50$ km s^{-1} cloud without much intervening extinction, its intensity at 10 pc is about 10^3 times the local interstellar field in the solar neighborhood. That flux is then at least as large as the UV flux from the local OB stars associated with the compact H II regions found by Ekers *et al.* (1983) and sufficient to account for the observed [C II] line flux (Lugten *et al.* 1986). In this scenario, the [C II] emission from the $+20$ km s^{-1} cloud is weaker since it is somewhat farther away from Sgr A West.

Another consequence of the likely location of the $+20$ and $+50$ km s^{-1} clouds in the inner 10 to 30 pc of the Galaxy is that there may then be a physical relationship of the circumnuclear disk between 1.5 and 6 pc from Sgr A* to a large nearby reservoir of gas. This is important as the circumnuclear disk would be a relatively short-lived feature ($\leq 10^6$ yr) unless material can be continuously fed into the central 5 pc (Güsten *et al.* 1987; Mezger *et al.* 1989; Ho *et al.* 1989).

b) Physical Conditions of the Molecular Gas near the Galactic Center

The relative weakness of the CO $7 \rightarrow 6$ line in the radio arc (§ III*d*), as well as in the $+20/+50$ km s^{-1} clouds (§ IV*b*), is puzzling. The gas kinetic temperatures and hydrogen densities consistent with all available CO measurements, $T_{\rm kin} \leq 40$ K and $n(H_2) \leq 10^4$ cm^{-3}, are significantly lower than estimated from CS, CH_3CN, and NH_3 data (Güsten *et al.* 1981, 1985; Morris *et al.* 1983; Armstrong and Barrett 1985; Serabyn and Güsten 1987). In addition, several components of $C^{18}O$ and CS emission in the radio arc and in the $+20/+50$ km s^{-1} clouds coincide with self-absorption dips in ^{12}CO lines (Fig. 5; Serabyn and Güsten 1987; Liszt, Sanders, and Burton 1975) that have brightness temperatures between 10 and 30 K. If the amount of gas indicated by the $C^{18}O$ line flux were at the temperatures and densities indicated by the NH_3 and CS measurements ($T_{\rm kin} \approx 50$–100 K, $n(H_2) \sim 3$ to 5×10^4 cm^{-3}) and had as large a filling factor as indicated by the ^{12}CO $1 \rightarrow 0$ line, one should observe a fully thermalized, optically thick CO $7 \rightarrow 6$ emission line of brightness temperature between ≈ 20 K (arc) and 40 to 80 K ($+20/+50$ km s^{-1} clouds). Assuming that temperatures of 40 K rather than 80 K are characteristic of the bulk of the gas in these clouds, the resulting heating requirements for the Galactic center clouds would then be about an order of magnitude less than assumed, for example, by Güsten *et al.* (1985).

Alternatively, the low ^{12}CO $7 \rightarrow 6$ brightness temperature may be consistent with the densities and temperatures estimated from the CS, NH_3, etc., data if the column density or filling factor of the warm dense gas were much smaller than those indicated by the low-J ^{12}CO data (High-Temperature, High-Density Model in Table 3). We have discussed in § III*e* the difficulties of this model to simultaneously account for ^{12}CO, $C^{18}O$, and ^{12}CO $7 \rightarrow 6$ lines. In this scenario, the ^{12}CO emission has a high filling factor and comes from pervasive warm, low-density interclump gas.

VI. CONCLUSIONS

We have presented observations of the $^2P_{3/2} \rightarrow {}^2P_{1/2}$ [C II] fine structure line, and of the ^{12}CO $3 \rightarrow 2$, $7 \rightarrow 6$, and $C^{18}O$ $2 \rightarrow 1$ rotational lines toward the radio arc and the $+20$ and $+50$ km s^{-1} clouds in the Galactic center. The measurements give new information on the location, physical conditions, and excitation of the interstellar gas clouds in the Galactic center.

Radio Arc.—[C II] and molecular line emission closely track the arched, thermal filaments of the radio arc. The bright [C II] emission probably comes from photodissociation regions at the surface of dense molecular clouds in the arc. About 2×10^4 $M_\odot$, or 10% of the entire mass of gas, is contained in C^+ regions, indicating the presence of an intense, pervasive far-ultraviolet radiation field ($\epsilon_{\rm uv} \geq 10^3$ $\epsilon_{\rm interstellar}$). Available models of *C*- or *J*-shocks cannot account for the large observed [C II] and far-infrared continuum luminosities. The most likely sources of the UV photons are several tens of distributed OB stars in or near the arc. These stars can plausibly account for the ionization in the filaments but need to be in a special geometry to explain the remarkable uniformity of the ionization over large scales.

$+20/+50$ km s^{-1} Clouds.—Our new observations indicate that the $+50$ km s^{-1} cloud, and thus by inference also the $+20$ km s^{-1} cloud, are within 15 pc of the Galactic nucleus. The $+50$ km s^{-1} cloud interacts with the nonthermal radio shell source Sgr A East and may be exposed to the ultraviolet radiation emanating from Sgr A West. Detection of high-velocity ($\Delta v \sim 100$ km s^{-1}) $C^{18}O$ emission toward Sgr A East for the first time gives direct kinematic evidence for a recent high-energy explosion ($E \sim 10^{52}$ ergs) in the center.

Physical Conditions in Galactic Center Clouds.—The relatively weak ^{12}CO $7 \rightarrow 6$ emission in the radio arc and the $+20/+50$ km s^{-1} clouds indicates that either the bulk of these molecular clouds has kinetic temperatures not exceeding 40 K and molecular hydrogen densities $\leq 10^4$ cm^{-3}, or that the low-J ^{12}CO emission comes from a pervasive component of warm, low-density interclump gas.

We are grateful to the staff of the Kuiper Airborne Observatory and of the United Kingdom Infrared Telescope for their excellent support. We thank A. Eckart and W. Wild whose contributions in the development of the MPE 350 GHz SIS receiver and in the observations at the IRAM 30 m telescope were essential. We thank K.-H. Gundlach and members of the IRAM Grenoble SIS Junction Laboratory for supplying the 350 GHz mixer junctions. We thank A. Sternberg, D. Downes, and H. Liszt for helpful discussions and comments and E. Erickson and A. Sternberg for communicating results prior to publication. We also are grateful to Mark Morris for a number of valuable comments. This research was in part supported by NASA grant NAG-2-208.

APPENDIX A

In order to investigate the physical parameters of the molecular gas in the Galactic center more quantitatively, we have constructed single-component models of the excitation and radiative transport of CO rotational emission. The models take into account the clumping of the gas. For simplicity we assume that the ^{12}CO, ^{13}CO, and $C^{18}O$ isotopes all arise in about the same region, although this assumption will in reality likely be violated to some extent. Cross sections for collisional excitation of CO by H_2 are taken from Flower and Launay (1985) and Schinke *et al.* (1985) and are also used for the excitation of the CO isotopes. In the first step of the model, the population of the CO rotational ladder is computed by solving the usual rate equations, taking into account line trapping in an iterative scheme. The radiative transport is approximated by a large velocity gradient formalism. We use the expression of the escape probability β as a function of line center optical depth τ_0 given by de Jong, Dalgarno, and Boland (1980)

$$\beta(\tau_0) = \begin{cases} [1 - \exp(-2.34\,\tau_0)]/(4.68\,\tau_0) : \tau_0 < 7 \\ \{4\tau_0[\ln(\tau_0/\sqrt{\pi})]^{1/2}\}^{-1} : \tau_0 \geq 7\,. \end{cases} \tag{A1}$$

This expression is appropriate for microturbulent gas.

The high spatial resolution observations by Serabyn and Güsten (1987) clearly show that the molecular material in the radio arc is clumpy. Large-scale area fitting factors and spectral profiles then depend on the opacities of the various transitions and isotopes. In the second step of our model, we therefore include the effects of clumping on line intensities and profiles. Our model follows Martin, Sanders, and Hills (1984), letting each clump have a Gaussian velocity profile of FWHM width $\Delta v_{\rm clump}$ (assumed to be 10 km s^{-1}). The ensemble of clumps has a macroturbulent, Gaussian velocity distribution with $\Delta v_{\rm cloud} > \Delta v_{\rm clump}$. In our calculations, we assume $\Delta v_{\rm cloud}/\Delta v_{\rm clump} \approx 3$ and an area filling factor per velocity interval ϕ_0 of 0.3 to 0.8. We also follow Martin, Sanders, and Hills (1984) in deriving the area filling factor for a given opacity by assuming Gaussian density profiles for individual clumps. The resulting Rayleigh-Jeans line brightness temperature as a function of velocity offset from line center v can be expressed as (Martin, Sanders, and Hills 1984)

$$T(v) = S(T_{\rm ex})\{1 - \exp[-\tau_{\rm eff}(v)]\}\,, \tag{A2}$$

where $T_{\rm ex}$ is the excitation temperature of the transition. The source function S is given by

$$S(T_{\rm ex}) = h\nu/k[\exp(-h\nu/kT_{\rm ex}) - 1]^{-1}\,. \tag{A3}$$

Martin, Sanders, and Hills have shown that for $\Delta v_{\rm cloud}/\Delta v_{\rm clump} \geq 3$ the effective optical depth can be approximately written as

$$\tau_{\rm eff}(v) = \phi_0\, A(\tau_0) \exp[-\pi(v/\Delta v_{\rm cloud})^2]\,. \tag{A4}$$

$A(\tau_0)$ gives the ratio of clump area filling factor to its geometrical area for a line center optical depth τ_0. The values of A for different clump density distributions can be found in Martin, Sanders, and Hills (1984). For $\Delta v_{\rm cloud}/\Delta v_{\rm clump} \leq 3$, equation (A4) is replaced by an integral formulation. The input parameters for the clumpy cloud model are $T_{\rm ex}$ and τ_0 which are taken from the excitation calculation.

Our model is probably the simplest approach that takes non–LTE excitation, radiative transport, clumpiness, and opacity-dependent filling factors into account. It is an improvement over simple single-component, homogeneous cloud models, but is neither fully self-consistent, nor completely physical. Radiative interactions between different clumps at the same velocity are neglected, as is the possible dependence of molecular excitation on position in each clump. Furthermore, there is in reality a range of densities and temperatures in the gas. The model gives, however, a first-order, average picture.

REFERENCES

Alfvén, H. 1954, *On the Origin of the Solar System* (Oxford: Oxford University Press).
Armstrong, J. T., and Barrett, A. H. 1985, *Ap. J. Suppl.*, **57**, 535.
Bally, J., Stark, A. A., Wilson, R. W., and Henkel, C. 1987, *Ap. J. Suppl.*, **65**, 13.
———. 1988, *Ap. J.*, **324**, 223.
Becklin, E. E., and Neugebauer, G. 1968, *Ap. J.*, **151**, 145.
Blundell, R., Carter, M., and Grundlach, K. H. 1988, *Internat. J. Infrared Millimeter Waves*, **9**, 361.
Brown, R. L., and Liszt, H. S. 1984, *Ann. Rev. Astr. Ap.*, **22**, 223.
Chernoff, D. F., Hollenbach, D., and McKee, C. F. 1982, *Ap. J. (Letters)*, **259**, L97.
Cox, P., and Laureijs, R. 1989, in *The Center of the Galaxy*, ed. M. Morris, (Dordrecht: Kluwer), p. 121.
Crawford, M. K., Genzel, R., Townes, C. H., and Watson, D. M. 1985, *Ap. J.*, **291**, 755.
de Jong, T., Dalgarno, A., and Boland, W. 1980, *Astr. Ap.*, **91**, 68.
Dent, W. A., Werner, M. W., Gatley, I., Becklin, E. E., Hildebrand, R. H., Keene, J., and Whitcomb, S. E. 1982, in *The Galactic Center*, eds. G. R. Riegler and R. D. Blandford (A.I.P. Conf. Proc., **83**), p. 33.
Draine, B. T. 1980, *Ap. J.*, **241**, 1021.
Draine, B. T., Roberge, W. G., and Dalgarno, A. 1983, *Ap. J.*, **264**, 485.
Ekers, R. D., van Gorkom, J. H., Schwarz, U. J., and Goss, W. M. 1983, *Astr. Ap.*, **122**, 143.
Erickson, E. F., Haas, M. R., Colgan, S. W. J., Simpson, J. P., Morris, M. R., and Rubin, R. H. 1989, in preparation.
Flower, D. R., and Launay, J. M. 1985, *M.N.R.A.S.*, **214**, 271.
Gatley, I., Becklin, E. E., Werner, M. W., and Harper, D. A. 1978, *Ap. J.*, **220**, 822.
Gatley, I., Becklin, E. E., Werner, M. W., and Wynn-Williams, C. G. 1977, *Ap. J.*, **216**, 277.
Genzel, R., Becklin, E. E., Wynn-Williams, C. G., Reid, M. J., Moran, D. T., Jaffe, D. T., and Downes, D. 1982, *Ap. J.*, **255**, 527.
Genzel, R., and Stacey, G. J. 1985, *Mitt. Astr. Ges.*, **63**, 215.
Genzel, R., and Townes, C. H. 1987, *Ann. Rev. Astr. Ap.*, **25**, 377.
Genzel, R., Watson, D. M., Crawford, C. M., and Townes, C. H. 1985, *Ap. J.*, **297**, 766.
Genzel, R., Harris, A. I., and Stutzki, J. 1989, in *Infrared Spectroscopy in Astronomy*, ed. M. Kessler and A. Glasse (ESA SP series), in press.
Genzel, R., *et al.* 1990, in preparation.
Goss, W. M., Anantharamiah, K. R., van Gorkom, J. H., Ekers, R. D., Pedlar, A., Schwarz, U. J., and Zhao, Jun-hui 1989, in *The Center of the Galaxy*, ed. M. Morris (Dordrecht: Kluwer), p. 345.
Güsten, R., and Downes, D. 1980, *Astr. Ap.*, **87**, 6.
Güsten, R., Walmsley, C. M., and Pauls, T. A. 1981, *Astr. Ap.*, **103**, 197.
Güsten, R., Walmsley, C. M., Ungerechts, H., and Churchwell, E. 1985, *Astr. Ap.*, **142**, 381.

Güsten, R., Genzel, R., Wright, M. C. H., Jaffe, D. T., Stutzki, J., and Harris, A. I. 1987, *Ap. J.*, **318**, 124.
Harris, A. I. 1986, Ph.D. thesis, University of California, Berkeley.
Harris, A. I., Jaffe, D. T., Silber, M., and Genzel, R. 1985, *Ap. J. (Letters)*, **294**, L93.
Harris, A. I., Jaffe, D. T., Stutzki, J., and Genzel, R. 1987, *Internat. J. Infrared Millimeter Waves*, **8**, 857.
Harris, A. I., Wild, W., Genzel, R., and Eckart, A. 1989, MPE technical report.
Heyvaerts, J., Norman, C., and Pudritz, R. 1988, *Ap. J.*, **330**, 718.
Hildebrand, R. H. 1983, *Quart. J.R.A.S.*, **24**, 267.
Ho, P. T. P., Jackson, J. M., Armstrong, J. T., and Szczepanski, J. C. 1989, *Bull. AAS*, **20**, 1018.
Hollenbach, D., and McKee, C. F. 1989, *Ap. J.*, **342**, 306.
Hollenbach, D., Tielens, A. A. W. G., and Takahashi, T. 1989, in preparation.
Liszt, H. S., Sanders, R. H., and Burton, W. B. 1975, *Ap. J.*, **198**, 537.
Lugten, J. B. 1987, Ph.D. thesis, University of California, Berkeley.
Lugten, J. B., Genzel, R., Crawford, M. K., and Townes, C. H. 1986, *Ap. J.*, **306**, 691.
Martin, H. M., Sanders, D. B., and Hills, R. E. 1984, *M.N.R.A.S.*, **208**, 35.
Mezger, P. G., Chini, R., Kreysa, E., and Gmünd, H.-P. 1986, *Astr. Ap.*, **160**, 324.
Mezger, P. G., Zylka, R., Salter, C. J., Wink, J. E., Chini, R., and Kreysa, E. 1989, *Astr. Ap.*, in press.
Morris, M., Polish, N., Zuckerman, B., and Kaifu, N. 1983, *Ap. J.*, **88**, 1228.
Morris, M., and Yusef-Zadeh, F. 1990, *Ap. J.*, submitted.
Okuda, H., *et al.* 1989, in *The Center of the Galaxy*, ed, M. Morris (Dordrecht: Kluwer), p. 281.
Pauls, T. A., Downes, D., Mezger, P. G., and Churchwell, E. 1976, *Astr. Ap.*, **46**, 407.
Reid, M. 1989, in *The Center of the Galaxy*, ed. M. Morris (Dordrecht: Kluwer), p. 37.
Sanders, R. H., and Lowinger, T. 1972, *A.J.*, **77**, 292.
Sandqvist, Aa., Karlsson, R., Whiteoak, J. B., and Gardner, F. F. 1987, in The Galactic Center, ed. D. Backer (AIP Conf., Proc., 155), p. 95.
Schinke, R., Engel, V., Buck, U., Meyer, H., and Diercksen, G. H. F. 1985, *Ap. J.*, **299**, 939.
Serabyn, E., and Güsten, R. 1987, *Astr. Ap.*, **184**, 133.
Sofue, Y., and Fujimoto, M. 1987, *Ap. J. (Letters)*, **319**, L73.
Stacey, G. J., Lugten, J. B., Genzel, R., and Townes, C. H. 1990, *Ap. J.*, submitted.
Stutzki, J., Stacey, G. J., Genzel, R., Graf, U. U., Harris, A. I., Jaffe, D. T., Lugten, J. B., and Poglitsch, A. 1989, in *Proc. Internat. Symp. Submillimetre and Millimetre Astronomy*, ed. A. S. Webster (Dordrecht: Kluwer), in press.
Thronson, H. A., and Harper, D. A. 1979, *Ap. J.*, **230**, 133.
Wannier, P. G. 1980, *Ann. Rev. Astr. Ap.*, **18**, 399.
Watson, D. M. 1984, in *Galactic and Extragalactic IR Spectroscopy*, ed. M. Kessler and J. Phillips (Dordrecht: Kluwer), p. 195.
Wink, J., Wilson, T. L., and Bieging, J. H. 1983, *Astr. Ap.*, **127**, 211.
Yusef-Zadeh, F. 1986, Ph.D. thesis, Columbia University.
Yusef-Zadeh, F. 1989, in *The Center of the Galaxy*, ed. M. Morris (Dordrecht: Reidel), p. 243.
Yusef-Zadeh, F., Morris, M., and Chance, D. 1984, *Nature*, **310**, 557.
Yusef-Zadeh, F., Telesco, C. M., and Decher, R. 1989, in *The Center of the Galaxy*, ed. M. Morris (Dordrecht: Kluwer), p. 287.

U. U. Graf, R. Genzel, A. I. Harris, N. Geis, A. Poglitsch, and J. Stutzki: Max-Planck-Institut für Physik und Astrophysik, Institut für extraterrestrische Physik, D-8046 Garching bei München, Federal Republic of Germany

G. J. Stacey and C. H. Townes: Department of Physics, University of California, Berkeley, CA 94720